IAC-14-C1.4.5

A DISTRIBUTED ATTITUDE CONTROL LAW FOR FORMATION FLYING BASED ON THE CUCKER-SMALE MODEL

Fabrizio Paita
IEEC & Universitat Politècnica de Catalunya, Spain, fabrizio@maia.ub.es

Gerard Gómez*, Josep J. Masdemont†

Abstract

In this paper we consider the attitude synchronization problem for a swarm of spacecrafts flying in formation. Starting from previous works on consensus dynamics, we construct a distributed attitude control law and derive analytically sufficient conditions for the formation to converge asymptotically towards a synchronized, non–accelerating state (possibly defined a priori). Moreover, motivated by the results obtained on a particular consensus model, first introduced by F. Cucker and S. Smale to modellize the translational dynamics of flocks, we numerically explore the dependence of the convergence process on the dimension of the formation and the relative initial conditions of the spacecrafts. Finally, we generalize the class of weights defined by the previous authors in order to dampen the aforementioned effects, thus making our control law suitable for very large formations.

I. INTRODUCTION

Formation flying is a well estabilished concept in the space community, with several missions relying on this approach having been planned (examples include Darwin and Proba 3 from ESA, TPF, Grace and Grail from NASA, and the Swedish Prisma project). Theoretically, groups of small, autonomous acting spacecrafts working in concert offer several advantages over single, monolithic ones, being not only cheaper, simpler and faster to build, but also, due to the inherent distributed structure of a formation, offering a greater mission stability, since the loss of a spacecraft does not necessarily compromise the efficiency of the entire formation. Moreover, formation flying opens up new mission possibilities, with optical interferometry probably being the most famous. The latter, which involves imaging reconstruction through super-imposition of data collected by different sources, has led to imagine formations (known as swarms) which are comprised of huge numbers of spacecrafts, and therefore are spread over surfaces which can be also hundreds of kilometers wide. To mention just one example, quite recently NASA has selected the "Orbital Rainbows" project (essentially, a cloud of dust–like spacecrafts acting as an adaptive optical imaging sensor) for a NIAC Phase II study.

One of the challenges of these formations lies in the design of control techniques, both for translational and attitude dynamics, which allow the spacecrafts to autonomously accomplish the tasks of guidance, navigation and control (for the translational context, interesting examples can be found in [1], [2], [3], [4]). In this paper we focus on the problem of attitude alignment (also known as synchronization), that is we want to design a control law that allows the spacecrafts to asymptotically achieve the same attitude and angular velocity. However, along the way, we will see how many concepts and solutions are very similar to those devised in the translational context. In this last regard, [5] and [6] offer a good general view on the matter.

In the literature, one of the simplest techniques developed to tackle this problem is the leader-follower approach ([7], [8]). In this, each follower of the formation simply tracks the attitude of a designated leader, thus offering the clear advantage of reducing the situation to well known tracking problems. However, with no back–up plans in tow, in this approach the leader becomes a single point of failure. As a natural evolution of this technique, in recent years several behavioral approaches ([9], [10]) have been developed. These involve designing the control torque as a function of the attitudes and angular velocities of the other spacecrafts in the formation (with the simplest case given by arranging the spacecrafts in a bidirectional ring [9]).

The approaches previously described can be collected under the big hat of consensus dynamics ([11]), and they arise from the great amount of work that has been done both on single and double integrator dynamics ([12], [13]). However, they generally focus on aspects related to the asymptotic convergence of the formation under the control torque, thus ignoring two aspects of this class of controls: the dependence of the convergence speed on the dimension of the formation and on the relative conditions among the agents. In this regard, a series of steps has been done starting from a consensus model introduced by F.

*IEEC & Universitat de Barcelona, Spain, gerard@maia.ub.es
†IEEC & Universitat Politècnica de Catalunya, Spain. josep.masdemont@upc.edu

Cucker and S. Smale back in 2007 to modellize the translational dynamics of flocks ([14], and also [15], [16], [17] for some of the improvements done on this model). Motivated by the results obtained for this model, the contribution of this paper is two–fold. First, we design a distributed attitude control law and we derive analytically sufficient conditions in order for the formation to asymptotically achieve attitude alignment, possibly with a customizable synchronization value. Secondly, we study numerically the dependencies previously described and we propose a dynamically changing definition for the feedback gains (inspired by the one of Cucker and Smale) in order to compensate for these effects. Additional simulations are performed to evaluate the goodness of our approach.

The remainder of the paper is organized as follows. In Section 2, we lay down some basic notations, regarding graphs and the associated matrix theory, that are used throughout the paper. Furthermore, by using the language previously introduced, we describe the Cucker–Smale model and some of the results associated. In Section 3, we introduce the notation used to describe the attitudes of spacecrafts and we design our control law, also proving our main analytical result. In Section 4, we present some simulations aimed to describe the characteristics of the convergence process associated with the control law introduced. Finally, in Section 5 we briefly summarize the results of the paper and individuate some directions for future work.

II. ANALYTICAL BACKGROUND

II.I Preliminary notions: graphs

In the previous section we have introduced the concept of consensus dynamics, that is the processes by which a collection of interacting agents achieve a common goal. A natural way to model the information flow that characterizes such dynamics is given by undirected/directed graphs. In the present subsection we present the notions associated to this topic that are used throughout the paper. A graphical example encompassing entirely these notions (and those at the beginning of the next subsection) is given in Figure 1.

First, we define a *graph* as a pair (X, Ω), where X is a finite non–empty set of indexed nodes (the agents) and Ω is a set of pairs of nodes, which we call *edges* (the links determining the communication structure of the formation). In an *undirected graph* these edges satisfy a symmetry property, that is if the nodes x_i and x_j are connected by an edge, then both nodes are passing information to the other. In contrast, in a *digraph* (directed graph) every edge has a direction determined by the order of the pair (e.g., (x_i, x_j) means that x_i is passing information to x_j but not vice-versa).

We say that a graph possesses a *path* if there exists a subset of Ω comprised of consecutive edges, that is there exists an ordered subset of edges $(x_{i_1}, x_{i_2}), (x_{i_2}, x_{i_3}), \ldots, (x_{i_{N-1}}, x_{i_N})$, with $\{i_1, \ldots, i_N\}$ denoting the indexes of the distinct nodes connected by the edges, where the order relation is determined by the first (parent) node of every edge being equal to the second (child) of the preceding one. We refer to this path as directed (undirected) if the corresponding graph is directed (undirected). Furthermore, we define as *root* the first node of the path.

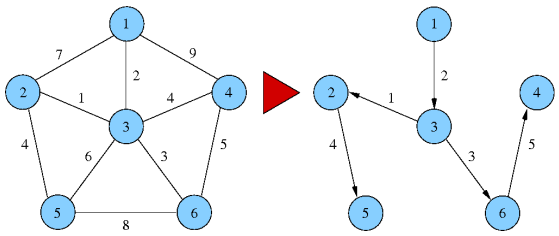

Figure 1: *Examples of weighted graphs, with an undirected connected one on the left and a directed one, possessing a directed spanning tree and derived form the first by assigning directions to the edges, on the right.*

Starting from the concept of path, it is possible to identify several ways in which the information flow spreads across the graph. In particular, we say that a directed (undirected) communication graph is *strongly connected* (*connected*) if there is a directed (undirected) path between any distinct pair of nodes. Moreover, we call *directed tree* a digraph where every node has exactly one parent, except for the root which we assume to have none. Finally, we say that a *directed spanning tree* of a digraph is a directed tree formed by edges that connect all the nodes in the graph. Obviously, such a structure is also a subgraph of the directed graph, that is a graph whose nodes set is a subset of the digraph one, and whose edges set equals that of the digraph restricted to the previous subset. Note that having a directed spanning tree is a weaker condition than being strongly connected, while in the case of an undirected graph the existence of an undirected spanning tree is actually equivalent to the graph being connected.

II.II Preliminary notions: matrices

Once a graph outlining the communication structure of a group of agents has been constructed, positive weights can be assigned to the edges of the graph in order to specify the strength of each edge. This kind of graph is known

as a *weighted graph*. Obviously, the notions introduced in the previous subsection can be applied to weighted graphs in a straightforward manner.

In order to catch in a unitary fashion all the informations embedded in a graph, it is useful to switch to the matrix language. In particular, we define the *adjacency matrix* $A = (a_{ij})$ of a weighted graph as the matrix whose entries are the weights assigned to the edges of the graph, with the rows corresponding to the parent nodes and the columns to the child ones. Furthermore, we define the *Laplacian matrix* $L = (l_{ij})$ associated to a weighted graph as the matrix with diagonal entries $l_{ii} = \sum_{j=1}^{N} a_{ij}$ and out–of–diagonal ones $l_{ij} = -a_{ij}$, with N denoting the number of nodes in the graph. Do note that the Laplacian matrix is symmetric positive definite in the case of undirected graphs. However, this is not true in the case of digraphs (where the matrix is non–symmetric).

The way in which the information spreads across the graph is obviously reflected in the spectral properties of the associated Laplacian matrix. In particular, in the case of an undirected communication graph, the Laplacian has a simple zero eigenvalue if and only if the graph is connected [18]. In the case of a digraph instead, the condition of the Laplacian possessing a simple zero eigenvalue is equivalent to the graph having a directed spanning tree [19]. In both cases, the eigenvector associated with the zero eigenvalue is the one having entries all equal to one. As we are going to see in the next section, these properties are crucial in order to construct a distributed control, both for translational and attitude dynamics.

Note that the previous statements hold regardless of the dimension of the space in which the agents live. That is, let x denote the vector $x = \left(x_0^T, \dots, x_N^T\right)^T$, where $x_i \in \mathbb{R}^m$. Then, under the conditions previously mentioned, $(L \otimes I_m)\, x = 0$ if and only if $x = \mathbf{1} \otimes \alpha$ (i.e, $x_0 = \cdots = x_N = \alpha$), with $\alpha \in \mathbb{R}^m$ and $\mathbf{1} = (1, \dots, 1)^T$ belonging to $\mathbb{R}^{(N+1)}$, and where $\otimes$ denotes the Kronecker product.

II.III The augmented Cucker–Smale model

In this subsection we introduce the model to be used as reference in the next section. While we describe this model in an unified fashion (in light of the language previously introduced), it is actually the sum of two different works, thus justifying the attribute "augmented" in the title. On one side we have the original paper of F. Cucker and S. Smale [14], where the case of an all–to–all communication structure (corresponding to an undirected connected graph) is analyzed, while on the other we have the work of J. Shen [15], which tweaks the original model in order to accommodate for a non–symmetric structure of the Laplacian and contains analytical results similar to those of Cucker and Smale.

Let x_i and v_i denote the three–dimensional position and velocity of the i–th element in a flock of $N+1$ agents. Then, the equations of motion for this agent under the augmented Cucker–Smale model (with the time dependence dropped for readability) can be written as

$$\dot{x}_i = v_i, \quad \dot{v}_i = -\sum_{j \in \mathcal{L}(i)} a_{ij} \left(v_i - v_j\right), \tag{1}$$

where the leadership sets $\mathcal{L}(i)$ and the weights a_{ij} determine respectively the communication structure and the edges weights associated to the underlying graph. Before defining them more precisely, let us transform the previous system in matrix form. By denoting with $x = \left(x_0^T, x_1^T, \dots, x_N^T\right)^T$ and $v = \left(v_0^T, v_1^T, \dots, v_N^T\right)^T$ the vectors whose components are respectively the positions and velocities of the agents, it is easy to check (see [14], for example) that the previous system can be rewritten as

$$\dot{x} = v, \quad \dot{v} = -L_x v, \tag{2}$$

where the operator L_x denotes the Laplacian operator acting on $\mathbb{R}^{3(N+1)}$ (or better, the Kronecker product of the Laplacian matrix with the three dimensional identity one). For brevity, we use this notations throughout the paper.

The distributed structure that we have defined before is rather standard for controls based on consensus dynamics [5]. However, two things distinguish the Cucker–Smale model from the rest. First, the weights a_{ij} are not constant, but are defined as

$$a_{ij}(t) = \frac{K}{\left(\sigma^2 + \|x_i(t) - x_j(t)\|^2\right)^{\beta}}, \tag{3}$$

where $K > 0$, $\sigma > 0$ and $\beta \geq 0$ are a given set of non-negative constants. In the context of the Cucker–Smale model, scaling the weights with respect to the relative distances between the agents, ensures that every agent pays more attention to the companions which are closest to it. We will see at the beginning of Section 4 how, in the context of attitude, this idea can be slightly tweaked in order to enhance consensus.

The second aspect lies in the leadership sets $\mathcal{L}(i)$. These can satisfy either $\#\mathcal{L}(i) = N$ (that is the case of a connected, undirected communication graph), or

- $a_{ij} \neq 0 \Rightarrow j < i$,
- $\forall i > 0,\ \mathcal{L}(i) \neq \emptyset$,

where the latter conditions define a hierarchical leadership for the flock in the following sense. If we look at the second condition, this is saying that every element in the flock has to communicate with someone. However , consider the natural order induced by the indexation of

the flock as $[0, 1, \ldots, N]$. Then, according to the first condition, every element i in the flock can communicate only with the elements j such that $j < i$ and it must do so at least with one of them. Do note that this is not true for the element 0 which, according to the second condition, acts independently from the rest of the flock, thus justifying the name of hierarchical leadership. When coupled, these conditions obviously imply the existence of a directed spanning tree, whose root is exactly the leader of the formation. Finally, from a control point of view, the presence of a hierarchical leadership serves two purposes: on one side, the presence of a leader (either real or virtual) ensures that a predefined trajectory for the formations to follow can be defined; on the other, it allows the formation to reach consensus with a low computational load for every spacecraft, due to the reduced number of connections among the agents.

The following result describes the main features of the augmented Cucker–Smale model and, indirectly, those of an entire class of controls.

Theorem 1. *Consider the equations of motion* (2)*. Then the following results hold:*

- *For $\beta < \frac{1}{2}$, global exponential convergence of the flock velocities to a consensus value is achieved both in the case of $\#\mathcal{L}(i) = N$ and in the presence of a hierarchical leadership*
- *For $\beta \geq \frac{1}{2}$ and $\#\mathcal{L}(i) = N$, the same exponential convergence is achieved under additional constraints on the initial conditions*

As a consequence, fixed values for the relative distances are reached exponentially fast. In addition, when a hierarchical leadership is present, it can be proved that the consensus velocity is indeed the one of the leader. For additional details, we refer the reader to [14] and [15].

It is worth to briefly look at least at the case $\#\mathcal{L}(i) = N$. If we define

$$\Lambda(t) = \frac{1}{2}\sum_{i \neq j} \|v_i - v_j\|^2, \tag{4}$$

then, for $\beta < \frac{1}{2}$ (and similarly for the other case), it results

$$\Lambda(t) \leq \Lambda(0) \exp^{-\frac{\nu K}{U_0^\beta} t}, \tag{5}$$

where U_0 is a function of the initial conditions and $\nu > \frac{1}{3(N+1)}$. The importance of this result lies in the fact that it arises directly from the properties of the Laplacian. In particular, the exponential convergence and the presence of the factor ν in the exponential are a direct consequence of the Laplacian being a symmetric, positive definite matrix, while the other factors are related to definition of the weights a_{ij}. This actually highlights the issues that we mentioned in the introduction, that is the dependence of the convergence process from the initial conditions and from the dimension of the flock are connaturated in the class of controls to which the model belongs. Of course, similar conclusions can be drawn for the non–symmetric case (though the analysis is much more difficult).

Before concluding, it is also worth mentioning that a result similar to the previous can be stated for discrete time (and of course a discrete model) and, additionally, consensus can be reached also in the presence of an accelerating leader [15] (provided the acceleration is decaying and not too great in magnitude with respect to the dimension of the formation).

III. ATTITUDE DYNAMICS

III.I Preliminaries

In this subsection we introduce some preliminaries and notations regarding attitude dynamics to be used in what follows. We use unitary quaternions $q = (\bar{q}, \hat{q})$ to describe the attitude of a spacecraft, with $\bar{q} = \cos\left(\frac{\theta}{2}\right)$ representing the scalar part of the quaternion and $\hat{q} = \hat{n}\sin\left(\frac{\theta}{2}\right)$ the vectorial part. The unitary vector $\hat{n}$ individuates the Euler axis, while θ denotes the instantaneous rotation angle about this axis. As well known, the same attitude can be represented by a quaternion q and its opposite. However, uniqueness can be achieved by restricting θ to the interval $0 \leq \theta \leq \pi$ so that $\bar{q} \geq 0$ [23].

The product of two unitary quaternions, which describes the composition of two rotations, is defined as

$$\overline{qp} = \bar{q}\bar{p} - \hat{q}\cdot\hat{p}, \quad \widehat{qp} = \bar{q}\hat{p} + \bar{p}\hat{q} + \hat{q}\times\hat{p}. \tag{6}$$

Of course, by definition, the product is still an unitary quaternion. Furthermore, we define the conjugate of a quaternion q as the quaternion $q^\star = (\bar{q}, -\hat{q})$. The latter describes the inverse rotation with respect to q, as it is easy to see from the fact that $q^\star q = qq^\star = \mathbf{q}_I$, where $\mathbf{q}_I = (1, 0, 0, 0)$. Finally, given two quaternions q and p, it results $(qp)^\star = p^\star q^\star$.

The attitude dynamics of a spacecraft can be described by the equations [23]

$$\begin{gathered}\dot{\bar{q}} = -\frac{1}{2}\omega\cdot\hat{q}, \quad \dot{\hat{q}} = -\frac{1}{2}\omega\times\hat{q} + \frac{1}{2}\bar{q}\omega, \\ I\dot{\omega} + \omega\times I\omega = \tau,\end{gathered} \tag{7}$$

where I denotes the tensor of inertia of the spacecraft, ω its angular velocity and τ the torque due to external and control forces. The dynamical equations are the so called Euler's equations, which describe the dynamics of

the spacecraft in its own principal frame, a rotating frame centered on the center of mass of the spacecraft and with axes parallel to the principal axes of inertia. In what follows, we assume that all the vectors mentioned are referred to the same reference frame.

III.II The control law

In this section we construct our distributed attitude control law and we prove that, under this law, a group of spacecrafts asymptotically achieve attitude synchronization. Before proceeding, it is worth to discuss some characterisitcs that distinguish the attitude consensus problem from its equivalents in situations modeled by standard single and double integrator dynamics [6] (take the augmented Cucker–Smale model described in the previous section as an example).

The greatest difference lies in the nonlinear kinematics of the problem. On one side, in order to achieve meaningful results, it is no longer possible to control just the velocities of the spacecrafts and then automatically achieve some bound on the relative positions, but both attitude and angular velocities need to be controlled in order for the spacecrafts to point in the same (specified) direction and to continue to do so during a certain time interval. On the other, the inherent non linear kinematics makes it difficult to repeat the qualitative analysis of the convergence process done by Cucker and Smale (and even more, that of Shen), even if, as we are going to see, a similar approach to prove the asymptotic convergence is adopted.

Another matter which is worth mentioning lies in the fact that the Cucker–Smale model has been designed in free space, while in our case (and more in general, throughout the astrodynamics field) we have a vector field to take into account. Since we are designing a continuous control, the easiest thing to do is to cancel the natural dynamics and add the control term itself. This is standard for feedback like controls and has sense in the context of attitude, where the relative conditions among the spacecrafts have more or less the same order of magnitude of their absolute ones. However (see [20] and [21] for a more extended discussion), attention must be paid when trying to apply this kind of strategy under the presence of different vector fields, and the dynamics exploited in order for the control to perform adequately.

In light of what has been discussed before we define the control torque for the i–th spacecraft as

$$\tau_i = \omega_i \times I_i \omega_i - I_i \sum_{j=0}^{N} g_{ij} \left[a_{ij} \widehat{q_j^\star q_i} + b_{ij} \left(\omega_i - \omega_j \right) \right], \tag{8}$$

where the weights a_{ij} and b_{ij} are real positive, while $g_{ij} = 1$ if agents i and j are connected by an edge and $g_{ij} = 0$ otherwise. Do note that, since our results are slightly more general than those of Shen, and Cucker and Smale, a different language has been used. Furthermore, as already stated, for now we do not give a precise definition of the weights. In the next section, we will see how we can define them in an advantageous way, starting from the idea of Cucker and Smale.

Before stating our theorem, we need a preliminary lemma in order to justify some of the computations. The proof of the theorem relies on the construction of a Lyapunov function, and the next lemma will be useful in order to construct such a function.

Lemma 1. *[22] If (q_i, ω_i) and (q_j, ω_j) satisfy the quaternion kinematics, then also $(q_i^\star q_j, \omega_i - \omega_j)$ 0 that. In addition, if $V_q = \|q_i^\star q_j - \mathbf{q}_I\|^2$, then $\dot{V}_q = (\omega_i - \omega_j) \cdot \widehat{q_j^\star q_i}$.*

With this lemma in tow, we are ready to prove asymptotic convergence for our control. We want to point out that part of the following theorem has been stated already in [22]. Here we observe how this theorem can be extended in order to accommodate for a wider range of situations, thus eliminating the need to modify the control law itself. Of course, also the proof can be found in [22]. We will limit ourselves to clarify and extend some points.

Theorem 2. *Consider the control torque defined by equation* (8)*. Furthermore, assume that one of the following hypotheses on the underlying communication graph hold true*

- *The graph is undirected and connected [22]*
- *The graph is directed and it possesses a directed spanning tree whose root does not receive informations from the other spacecrafts*

Then, there exist $\tilde{q}$ and $\tilde{\omega}$ such that $q_i \to \tilde{q}$ and $\omega_i \to \tilde{\omega}$, $\forall i \in \{0, \ldots, N\}$.

Before proceeding with the proof, some things should be noted. First of all, while for applications we will continue to work with the communication structures introduced along with the augmented Cucker–Smale model, we want to point out that the previous theorem actually encompasses a slightly more general class of communications. Furthermore, in [22] it is requested for the cardinality of the edges set to be at most equal to the dimension of the formation. While not explicitly stated in that paper, this is clearly a minimal hypothesis (valid also in the case of a digraph, but with only N edges), which (along with the connection) is simply stating that the information flow needs to reach every spacecraft in order for them to synchronize on the same value. With that said, we can proceed with the proof.

Proof. The proof rests on the LaSalle's invariance principle. Consider the Lyapunov function candidate

$$V = \frac{1}{2}\sum_{i,j=0}^{N} g_{ij}a_{ij}\|q_j^\star q_i - \mathbf{q}_I\|^2 + \frac{1}{2}\sum_{i=0}^{N}\|\omega_i\|^2. \quad (9)$$

By keeping in mind the expression (8) of the control torque, from Lemma 1 the derivation of the function (III.II) yields (see [22] for more details)

$$\dot{V} = -\frac{1}{2}\sum_{i,j=0}^{N} g_{ij}b_{ij}\|\omega_i - \omega_j\|^2 \leq 0. \quad (10)$$

Do note that, since $\dot{V}$ does not depend from the q_i's, it is not possible to apply directly Lyapunov's second criterion.
Now, let $\Gamma = \left\{\left(q_j^\star q_i, \omega_i\right) | \dot{V} = 0\right\}$. Also, let $\bar{\Gamma}$ be the largest invariant set contained in Γ. Obviously, on $\bar{\Gamma}$ it results $\dot{V} = 0$, which in turn implies $\omega_i = \omega_j$, $\forall i, j$. This follows from the weights b_{ij} being strictly positive and the connection hypotheses that we made. As a consequence, we see that $\dot{\omega}_i = \dot{\omega}_j$, and therefore the vector $\omega = (\omega_0, \ldots, \omega_N)$ can be written as $\omega = \mathbf{1} \otimes \eta$, with $\eta \in \mathbb{R}^3$.

Now, in the case of a digraph the hypothesis of the root (leader) being isolated implies $\dot{\omega}_0 = 0$. This is because either the root is cancelling its natural acceleration or it is not moving at all (which probably corresponds to the case of a virtual state to track). As a consequence of what has been said before, this implies that all the other derivatives are zero on $\bar{\Gamma}$.

In the case of an undirected connected graph instead, since $\omega_i = \omega_j$, it follows from the controlled equations of motion that

$$\dot{\omega}_i = -\sum_{j=0}^{N} g_{ij}a_{ij}\widehat{q_j^\star q_i}, \quad i = 0, \ldots, N. \quad (11)$$

We also know that

$$\sum_{i=0}^{N}\eta\cdot\dot{\omega}_i = -\sum_{i=0}^{N}\eta\cdot\left(\sum_{j=0}^{N} g_{ij}a_{ij}\widehat{q_j^\star q_i}\right) = 0, \quad (12)$$

since the graph is connected and $\widehat{q_j^\star q_i} = -\widehat{q_i^\star q_j}$. Therefore, since $\dot{\omega}$ is orthogonal to η, it results that $\dot{\omega}_i = 0, \forall i$. In both cases, we can therefore state that

$$\sum_{j=0}^{N} g_{ij}a_{ij}\widehat{q_j^\star q_i} = 0, \quad i = 0, \ldots, N. \quad (13)$$

It is easy to see [24] that the previous expression can be rewritten in matrix form as

$$(L \otimes I_3)\,\hat{q}_l = 0, \quad (14)$$

with I_3 denoting the three dimensional identity matrix, $\otimes$ the Kronecker product, $\hat{q}_l = \left(\hat{q}_0^T, \ldots, \hat{q}_N^T\right)^T$ and $L = (l_{ij})$ being the Laplacian with diagonal entries $l_{ii} = \sum_{j=0}^{N} g_{ij}a_{ij}\bar{q}_i$ and out of diagonal ones $l_{ij} = -g_{ij}a_{ij}\bar{q}_i$. From our hypotheses (and the unitarity of the quaternion) follows directly $q_i = q_j, \forall i, j$. Finally, the thesis follows by applying the LaSalle's invariance principle. □

Before concluding, we want to point out that the set $\bar{\Gamma}$, in the case of the second hypothesis, obviously shrinks down to the coordinates of the root, thus proving that this point is an asymptotically stable equilibrium.

IV. NUMERICAL SIMULATIONS

IV.I Preliminaries

In this subsection we give an introduction to the simulations performed with the designed control, explaining how they are done and what are their specifics.
The main purpose of these simulations is to understand the performance of the control defined in equation (8) (both with constant weights and CS–like weights) under some real life limitations, in particular a maximal value for the torque applied. This analysis is carried out mainly as a function of the convergence time since, as we are going to show in the next subsections, this quantity is sensible to many others, in particular to the dimension of the formation.

Regarding the specifics of the simulations, the first thing that needs to be mentioned lies in the definition of the weights a_{ij} and b_{ij}. We have seen in Theorem 3.1 that a sufficient condition for asymptotic convergence is for the weights to be strictly positive. However, as seen for the Cucker–Smale model, something more can be done. In particular, in the context of that model, it can be observed that the weights are increasing for decreasing relative distance, that is if

$$\|x_i(t) - x_j(t)\| \leq \|x_i(\bar{t}) - x_j(\bar{t})\|, \quad (15)$$

for certain $t, \bar{t} \in \mathbb{R}$, then

$$a_{ij}(t) = \frac{K}{\left(\sigma^2 + \|x_i(t) - x_j(t)\|^2\right)^\beta} \geq a_{ij}(\bar{t}). \quad (16)$$

In the context of attitude, this behaviour can be exploited in order to increase the convergence rate, especially for a great number of spacecrafts, where, as shown by the Cucker–Smale model, the convergence may become quite slow for large dimensions. In fact, it is easy

to observe that, since our objective lies in attitude synchronization (that is we want to bring to zero relative attitudes and angular velocities), replacing the relative distance with a scaling factor which goes to zero at consensus can be used to increment the convergence rate due to the increasing of the weight value as consensus approaches. Of course, this scaling factor should be related in some way to the linear term that accompanies the weight.

For example, the results presented in this section assume two different scaling factors for the weights a_{ij} and b_{ij}. In the first case, we take as scaling factor the instantaneous rotation angle given by the quaternions. According to the notations of Section 3.1, the weights will then read as

$$a_{ij}(t) = \frac{K}{(\sigma^2 + \|\theta_i(t) - \theta_j(t)\|^2)^{\beta}}. \qquad (17)$$

This choice reflects the fact that, while in the control itself we are just working with the vector part of the relative quaternion, as a consequence of the unitarity, the scalar parts of the quaternions referred to the agents will achieve asymptotically the same value. Do note that, due to the ambiguity inherent in the quaternions, we have avoided using the scalar part itself (which may end up giving the effect opposite to the one intended).

For the angular velocities instead, assuming a spherical coordinates point of view, either the polar or the azimuthal angle can be chosen (remember that we are assuming all the vectors described in the same reference frame). This choice is due, of course, to the fact that, as consensus approaches, the angular velocity vectors will lie on the same line. In particular, we use the azimuthal angle in Section 4.2 and the polar one in Section 4.3. Do note however that no explicit comparison between the two choices has been done, since it lies beyond the goals of this paper (although it is expected that using the angle corresponding to a minimum axis of inertia may yield better results than the other one, due to the increased rate of convergence along that direction).

Finally, all the simulations that we present here have a couple of common elements. First of all, they are all conducted assuming that the formations considered are comprised of standard 3U–cubesats ($10 \times 10 \times 30$ cm, 4 kg). Secondly, unless differently noted, the initial conditions for the simulations are randomly generated following an uniform distribution appropriate for the simulation performed (except for the first spacecraft, which is assumed always having coordinates $q_0 = (1, 0, 0, 0)$ and $\omega_0 = (0, 0, 0)$). In particular, a custom made C routine, based on the functions *rand()* (modified to generate real numbers in an interval) and *srand()*, has been employed to generate these random initial conditions, with the seed for the *srand()* function chosen semi–randomly through the *time(NULL)* instruction. However, the initial conditions used have been stored and can be provided on request.

That said, for every simulation, the values of the weights in the constant case are selected in order to be equal to those of the CS–like case at the initial time, so to allow for a precise estimation of the efficiency of the adaptive process in weights definition. As a last note, convergence to a synchronized state is assumed achieved in the plots when, both for attitudes and angular velocities, all the spacecrafts are inside a cube of side 10^{-4}.

In what follows, first we are going to analyze the case $N = 2$, where a complete description (in terms of initial relative conditions) of the convergence rate is possible. We will then move to the case $N > 2$, where the dimension and the underlying communication graph take the lead role in affecting the convergence rate. Explanations on relevant details for the generation of the plots are provided in pointed lists.

IV.II The two dimensional case

In this subsection we are going to briefly analyze the case of two spacecrafts (subject to the dynamics defined in (7) and the control torque (8)) synchronizing under the effects of an undirected communication graph. We will see in the next subsection what happens in the other case.

Without imposing any limitation on the control torque, the analysis is pretty straightforward and it essentially involves understanding only a couple of concepts.

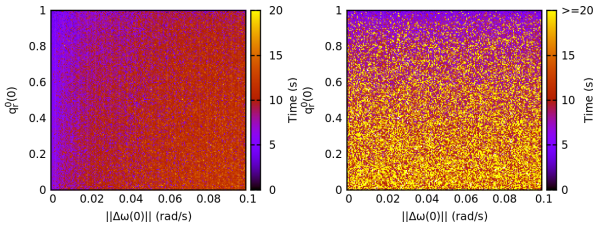

Figure 2: *Convergence time comparison between CS–like weights (left) and constant ones (right) for a two spacecraft formation under an undirected communication graph. The weights parameters are $K = 5$, $\sigma^2 = 10^{-2}$ and $\beta = 0.4$. Details on how to generate these plots can be found in the pointed list of Section 4.2.*

First of all, let's look at Figure 2. In these plots we represent the convergence time for the control (constant weights on the right, CS–like on the left) in terms of the relative attitude (denoted by the scalar part of the relative quaternion on the y axis) and angular velocity (x axis) between the spacecrafts. For every couple $\left(q_r^0(0), \|\Delta\omega(0)\|\right)$, initial conditions are generated anew in the following manner:

- Starting from the values of $\sqrt{1-\left(q_r^0\left(0\right)\right)^2}$ and $\|\Delta\omega\left(0\right)\|$, random values along the three axes, comprised between these values and their opposite, are generated through the modified *rand()* routine described in the previous section;
- The norms corresponding to the vector part of the quaternion and the angular velocity defined by these quantities are then computed, and the latter vectors are normalized by dividing the components for these norms;
- Multiplication of the components by the nominal norms ($\sqrt{1-\left(q_r^0\right)^2}$ and $\|\Delta\omega\left(0\right)\|$) finally follows to achieve the conditions used in the simulations;
- The values of $q_r^0\left(0\right)$ and $\|\Delta\omega\left(0\right)\|$ are then updated with steps 5×10^{-3} for the quaternion and 5×10^{-4} for the angular velocity (starting value is 0 in both cases).

Now, if we look at the plot on the left, we can observe that, in general, the closer the spacecrafts are in terms of relative attitude and angular velocity, the faster is the convergence. However, there is a quite significant random component (which can be observed if one look at the values for either a fixed relative attitude or a fixed relative angular velocity) in the specific values of the convergence times. This seem to be mainly due to the fact that there is a minimum axis of inertia, which determines a direction where the convergence of the control is faster. In addition, if we now consider also the plot on the right, it can be noted that constant weights, besides offering a worse performance than the CS–like weights (the convergence time can in fact surpass the 60 seconds, although the plot is cut at 20 for comparative reasons), also seem to cause the convergence to be mainly affected by the relative attitude between the spacecrafts.

Finally, as we can see on the left of Figure 3, the advantage in convergence velocity offered by the CS–like weights, is achieved at the expense of a control torque that exceeds the capabilities of a $3U$–cubesat. However, this problem can be easily avoided by modifying the feedback gains. Of course, as can be seen in the plots on the right of Figure 3, reducing the magnitude of the weights lowers the amount of torque required, but also leads in general to a slower convergence, which is also characterized by an increased number of oscillations around the convergence state.

IV.III The case $N > 2$

In the previous subsection we have seen the behaviour of a formation comprised of only two spacecrafts. In this one instead, we investigate what happens in the case $N > 2$. In light of the random element outlined in the previous subsection, this analysis is conducted through the use of a series of Monte–Carlo simulations.

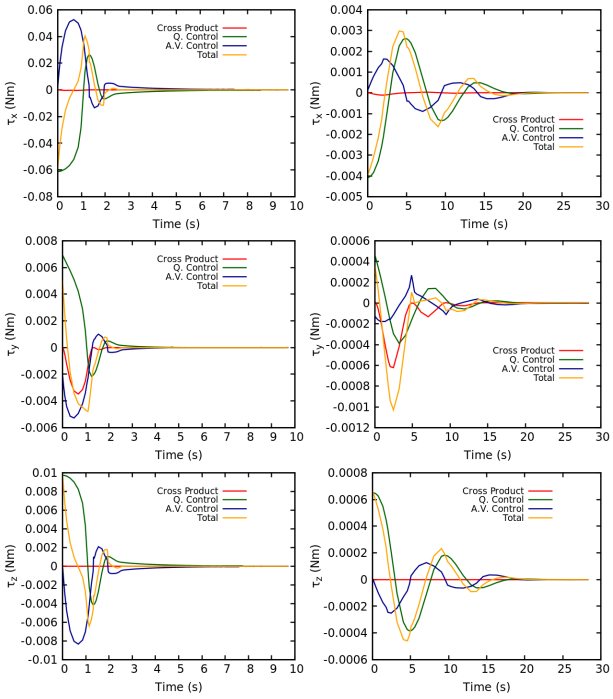

Figure 3: *Comparison between the torques for CS–like weights with the parameters defined before (left) and a new set ($K = 0.5$, $\sigma^2 = 1$ and $\beta = 5.5$). The initial conditions correspond to those of Figure 2 associated to $q_r^0\left(0\right) = 0.9$ and $\|\omega\left(0\right)\| = 0.05$. From top to bottom, the torques corresponding to the x, y and z axis are depicted. In orange we have the total torque while for the rest, following the colors order in the plots, we have the contributions of the natural dynamics, the quaternions control term and the corresponding angular velocities one.*

As a starting point, additional informations are in order so to understand the plots presented here. In particular, the initial conditions are the same for all the plots in this section and are generated in the following manner:

- As stated in Section 4.1, the first spacecraft is always assumed having coordinates $q_0 = (1, 0, 0, 0)$ and $\omega_0 = (0, 0, 0)$;
- As for the rest, let $\bar{N}$ denote the maximal dimension for the plots. Then, for every value of N, a value for $\bar{q}\left(1-\left(N/\bar{N}\right)\right)$ and one for $\|\omega\|\left(10^{-1}\times\left(N/\bar{N}\right)\right)$ are selected and 2500 corresponding initial conditions are generated in the same way of the previous

section (although in this case quaternion and angular velocity are absolute quantities and not relative ones);

- Additionally, for a growing N, the conditions generated up to $N-1$ are retained and the simulations are performed with different underlying communication graphs;

- For every dimension, the convergence times are obtained from the average of the convergence times corresponding to the various initial conditions. The latter means that, of the 2500 sets of initial conditions per spacecraft, the first for every spacecraft is collected and together they are used to compute a convergence time; the same is then done for the second, the third and so on, and the average is then done on these times.

In addition, a maximal time of convergence has been imposed and, correspondingly, a certain maximal amount of simulations (250 for the plots in Figure 6, 100 for the rest) exceeding this time is allowed in order to catch extremal conditions due to the different growing of the various graphs (with the average done on the conditions that do not exceed the maximal time allowed). In conclusion, we want to point out that the choice for the initial conditions previously described is not casual, but it arises from what has been observed in the two dimensional case. In fact, in that situation we have observed that closeness brings faster convergence times, so it is only natural to ask if the same can be said for an arbitrary dimension (of course, keeping in mind that the number of factors to take into account has increased).

Now, let's look at Figure 4. In the plots, no limitations on the torque magnitude have been imposed. The communication structures instead are defined a s follows:

- "Full" corresponds to an all–to–all communication (and therefore to a simple synchronization individuated by an undirected communication graph);

- The others use the first spacecraft (which again, may also represent only a state to track) as a leader, while the rest of the spacecrafts communicate with a certain number of their companions preceding them in the indexation of the formation.

- This number is either a maximal one (indicated in the plot and with "Chain" corresponding to 1) or the number of preceding spacecrafts available.

The previous choices help us to describe what is the performance of the control with a formation that is increasingly spread across space (so much so, that the number of available spacecrafts from which deriving data for the synchronization may drop up to one spacecraft only).

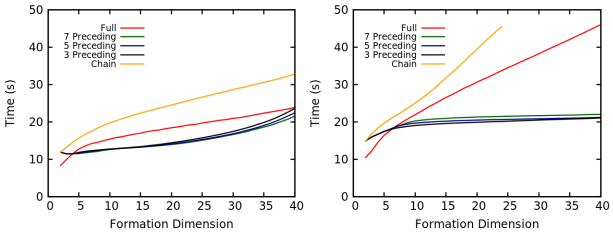

Figure 4: *Convergence time with respect to formation dimension for different communication structures using CS–like weights (left) and constant ones (right) without restriction on the torque magnitude. The weights parameters are $K = 2$, $\sigma^2 = 10^{-2}$ and $\beta = 0.4$, while the maximal convergence time is 60 seconds. See the first pointed list of Section 4.3 for how the initial conditions have been generated and the paragraph below for an explanation of the different structures.*

The first thing that it's interesting to note is the fact that, both for CS–like weights and constant ones, there appears to be a sharp difference among the communication structures, with the ones possessing a leader (with the notable exception of "Chain") tightly grouped on the bottom parts of the plots and performing better than a simple synchronization. Furthermore, it can be noted that, in the plot for constant weights, all the graphs exhibit the same concavity. However, for the CS–like weights, this concavity changes for some of the graphs, seemingly indicating an excessive push given by the weights for dimensions greater than 40. However, further analysis (at least up to the second derivative and for greater dimensions) is required in order to draw more meaningful conclusions.

Clearly, when a limitation on the torque magnitude is imposed, this behaviour changes drastically. In Figure 5 (next page), we have calculated again the convergence times of Figure 4, but with an additional constraint on the magnitude of the torque (which cannot exceed 1 mN). As expectable, both for CS–like weights (left) and for constant weights (right), the convergence times increase drastically, since the control cannot express its full capability. That said however, a clear advantage given by the use of the scaled weights in place of the constant ones can be observed. In particular, let's look at the plot with constant weights. Obviously (and this is true also for the behaviours observed in the previous paragraph), in this case there is no damping effect given by the scaling. Therefore, it can be inferred with reasonable certainty that the behaviour of the profiles associated with the various communication structures is due to the particular structure of the control law (see the example of Section 2.1). Scaling

the weights slows down this behaviour, and it is easy to guess that, for greater dimensions, its importance is even more pronounced due to the different growings observed when using the same communication structures.

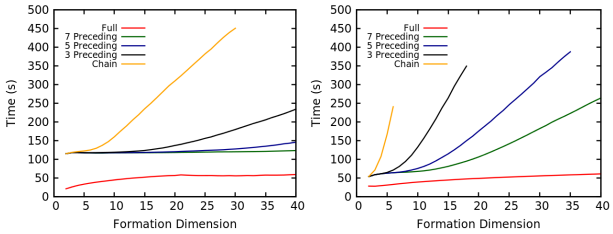

Figure 5: *Convergence time with respect to formation dimension for different communication structures using CS–like weights (left) and constant ones (right), with an imposed maximal torque magnitude of* 1 *mN. The weights parameters are* $K = 0.5$, $\sigma^2 = 10^{-2}$ *and* $\beta = 0.4$, *while the maximal convergence time is* 600 *seconds. The plots are generated in the same way of Figure 4.*

A second point that can be observed is the dependence from the communication structures. In particular, differently from what happened in the case with no limitation on the torque magnitude, it seems that the "fullest" is the communication structure (in the sense of a growing number of parent nodes for a child one) the lower is the convergence time. Furthermore, it can be observed that, both for constant weights and CS–like weights, there is a distinct difference between the "Full" profile (which is very similar in the two cases) and the other ones (besides the damping effect previously described). This actually seems to indicate that an all–to–all communication structure is solid enough to not require any improvement to obtain reasonable convergence times, which however becomes fundamental when weaker communication structures (especially for very large formations) are employed due to the natural stretching of a formation over a large surface and/or in order to decrease the computational load for the spacecrafts.

V. CONCLUSION

In the present paper we have proposed a distributed attitude control law aimed to achieve attitude synchronization among spacecrafts belonging to a formation. We have studied analytically under which conditions this goal is reached. Motivated by the work of F. Cucker and S. Smale, we have also analyzed numerically the dependence of our control law from the dimension of the formation and the relative initial conditions of the spacecrafts. Finally, following again the work of the previous authors, we have proposed a scaling of the feedback weights in order to compensate for the previously outlined dependencies. The simulations performed show the goodness of our approach in order to design a control law suitable for swarms of spacecrafts.

Do note however, that a question remains for the case $N > 2$. The initial conditions for the spacecrafts have been selected in order for the latter to be very close to each other in terms of relative attitude and angular velocity with respect to the communication structures employed. Is this again an optimal configuration in terms of convergence time, as in the case $N = 2$? What happens when, keeping fixed the values of attitude and angular velocity for every spacecraft (and therefore the associated initial conditions), we switch the positions of the spacecrafts in the formation in order to modify the relative data? In future works we aim to answer (at least) these questions.

VI. ACKNOWLEDGEMENTS

Fabrizio Paita has been supported by the PITN-GA-2011-289240 European program. Furthermore, G.G. thanks the Catalan government for the grant SGR 115 and the Spanish one for the grant MTM2013-41168-P. Finally, J.J.M. thanks the MINECO-FEDER for the grant MTM 2012-31714 and the Catalan government for the grant 2009 SGR-D-D589-E.

References

[1] C.R. McInnes. Potential Function Methods for Autonomous Spacecraft Guidance and Control. *Astrodynamics 1995: Proceedings of the AAS/AIAA Astrodynamics Conference, Halifax, Canada. 1996.*

[2] L. García-Taberner, J.J. Masdemont. FEFF methodology for spacecraft formations reconfiguration in the vicinity of libration points *Acta Astronautica, Vol. 67, No. 7-8, pp. 810-817, October-November 2010.*

[3] G. Gómez, M. Marcote, J.J. Masdemont, J.M. Mondelo. Zero Relative Radial Acceleration Cones and Controlled Motions Suitable for Formation Flying *Journal of the Astronautical Sciences, Vol. 53, No 4, pp. 413-431, October-December 2005.*

[4] G. Mingotti, C. McInnes. Relative Orbital Dynamics of Swarms of Femto-Spacecraft. *64th International Astronautical Congress, Beijing, China, September 2013.*

[5] W. Ren, Y. Cao. Distributed Coordination of Multiagent Networks. *Communication and Control Engineering Series, Springer-Verlag, London, 2011.*

[6] W. Ren, R.W. Beard. Distributed Consensus in Multi-vehicle Cooperative Control. *Communication and Control Engineering Series, Springer-Verlag, London, 2008.*

[7] P.K.C. Wang, F.Y. Hadaegh. Coordination and Control of Multiple Microspacecraft Moving in Formation. *Journal of the Astronautical Sciences, Vol. 44, No. 3, pp. 315-355, July-September 1996.*

[8] P.K.C. Wang, F.Y. Hadaegh, K. Lau. Synchronized Formation Rotation and Attitude Control of Multiple Free-flying spacecraft. *AIAA Journal of Guidance, Control and Dynamics, Vol. 22, No. 1, pp. 28-35, January-February 1999.*

[9] J.R. Lawton, R.W. Beard. Synchronized Multiple Spacecraft Rotations. *Automatica, Vol. 38, No. 8, pp. 1359-1364, August 2002.*

[10] W. Ren, R.W. Beard. Decentralized Scheme for Spacecraft Formation Flying via the Virtual Structure Approach. *AIAA Journal of Guidance, Control and Dynamics, Vol. 27, No. 1, pp. 73-82, January 2004.*

[11] T. Vicsek, A. Zafeiris. Collective motion. *Physics Reports, Vol. 517, No. 3-4, pp. 71-140, August 2012.*

[12] L. Moreau. Stability of Multi-agent Systems with Time-dependent Communication Links. *IEEE Transactions on Automatic Control, Vol. 50, No. 2, pp. 169-182, February 2005.*

[13] R. Olfati-Saber. Flocking for Multi-agent Dynamic Systems: Algorithms and Theory. *IEEE Transactions on Automatic Control, Vol. 51, No. 3, pp. 401-420, March 2006.*

[14] F. Cucker, S. Smale. Emergent Behavior in Flocks. *IEEE Transactions on Automatic Control, Vol. 52, No. 5, May 2007.*

[15] J. J. Shen. Cucker–Smale Flocking Under Hierarchical Leadership. *SIAM Journal on Applied Mathematics, Vol. 68, No. 3, 2008.*

[16] J. Park, H.J: Kim, S.Y. Ha. Cucker–Smale Flocking With Inter–Particle Bonding Forces. *IEEE Transactions on Automatic Control, Vol. 55, No.11, November 2010.*

[17] S. Motsch, E. Tadmor. A New Model for Self–organized Dynamics and Its Flocking Behavior. *Journal of Statistical Physics, Vol. 144, No. 5, pp. 923-947, September 2011.*

[18] F.R.K. Chung. Spectral Graph Theory. *Regional Conference Series in Mathematics, American Mathematical Society, Providence, 1997.*

[19] W. Ren, R.W. Beard, T.W. McLain. Coordination Variables and Consensus Building in Multiple Vehicle Systems. *Lecture Notes in Control and Information Science, Vol. 309, pp. 171-188, 2005.*

[20] L. Perea, G. Gómez, P. Elosegui. Extension of the Cucker–Smale Control Law to Spaceflight Formations. *Journal on Guidance, Control and Dynamics, Vol. 32, No. 2, March–April 2009.*

[21] F. Paita, G. Gómez, J.J. Masdemont. On the Cucker–Smale Model Applied to a Formation Moving in a Central Force Field. *64th International Astronautical Congress, Beijing, China, September 2013.*

[22] W. Ren. Distributed Attitude Alignment in Spacecraft Formation Flying. *International Journal of Adaptive Control and Signal Processing, Vol. 21, No. 2-3, pp. 95-113, March-April 2007.*

[23] P.C. Hughes. Spacecraft Attitude Dynamics. *Wiley, New York, 1986.*

[24] W. Ren. Distributed Attitude Consensus Among Multiple Networked Spacecraft. *Proceedings of the 2006 American Control Conference, Minneapolis, June 2006.*